PAPER

Performance Evaluation of SeaSonde High-Frequency Radar for Vessel Detection

AUTHORS

Hugh J. Roarty
Erick Rivera Lemus
Ethan Handel
Scott M. Glenn
Coastal Ocean Observation Laboratory, Rutgers University

Donald E. Barrick
James Isaacson
CODAR Ocean Sensors, Ltd., Mountain View, CA

ABSTRACT

High-frequency (HF) surface wave radar has been identified to be a gap-filling technology for Maritime Domain Awareness. Present SeaSonde HF radars have been designed to map surface currents but are able to track surface vessels in a dual-use mode. Rutgers and CODAR Ocean Sensors, Ltd., have collaborated on the development of vessel detection and tracking capabilities from compact HF radars, demonstrating that ships can be detected and tracked by multistatic HF radar in a multiship environment while simultaneously mapping ocean currents. Furthermore, the same vessel is seen simultaneously by the radar based on different processing parameters, mitigating the need to preselect a fixed set and thereby improving detection performance.

Keywords: radar, detections, maritime domain awareness, dual-use

Introduction

The U.S. Integrated Ocean Observing System (IOOS®) led by the National Oceanic and Atmospheric Administration (NOAA) has designed (Interagency Working Group on Ocean Observation, 2009), is constructing, and has recently begun operating the more advanced portions of a national high-frequency (HF) radar network focused on the real-time mapping of surface currents. The primary operational users of the resulting surface current maps are the U.S. Coast Guard for Search and Rescue and the NOAA HazMat team for ocean spill response. The IOOS Mid-Atlantic Region's CODAR SeaSonde HF Radar Network, led by Rutgers University, is the first region in the United States to achieve operational status by constructing and operating the end-to-end system that produces and links validated real-time surface current maps to the Coast Guard's Search and Rescue Optimal Planning System (Roarty et al., 2010b).

The Department of Homeland Security has called for the development of tools to provide wide-area surveillance from the coast to extend beyond the horizon (Department of Homeland Security Science and Technology, 2009). Rutgers and CODAR Ocean Sensors, an academic-industry partnership established in 1997, have worked together for over a decade to expand the capabilities of compact CODAR HF radars to include the dual-use application of detecting and tracking ships without compromising the network's ability to map surface currents. Initial development focused on the demonstration and evaluation of a non-real-time end-to-end system for dual-use vessel tracking in the New York Bight multifrequency HF radar testbed (Roarty et al., 2010a). Technology demonstrations determined (a) that vessels could be detected, (b) that multilook detections could be associated with a known ship, and (c) that the associated detections could then be input to a range of tracking algorithms whose output produced tracks and predicted trajectories on a computer screen, providing useful information to operators. Radar hardware development focused on developing network flexibility beyond monostatic backscatter operations, demonstrating (a) that bistatic and multistatic operations were possible with a shore-based network and (b) that buoy-based bistatic transmitters can be operated at all three of the commonly used HF radar frequencies (5-6, 12-13, and 24-25 MHz). The greatest challenge in developing a robust ship surveillance capability for any HF radar is the development of the initial vessel detection algorithm. This conclusion focused the initial research on the mathematical problem of identifying and extracting the radar return of a surface vessel hidden within a highly variable and noisy background, requiring additional detection algorithm development, testing, and sensitivity analysis in a variety of environments with different noise characteristics. It is the aim of this paper to

analyze the parameters and settings of the vessel detection algorithm that are optimal for finding those ship echoes among the other signals that are sent back towards the radar. In Methodology, we describe the HF radar network, the SeaSonde HF radar used in this test, the Automatic Identification System (AIS) network used to ground truth the radar detections, and the ship detection software used to process the radar data for ships. In Results, we discuss the results of the ship detection test that was conducted. Lastly, the performances of the various ship detection processing methods against the available targets are discussed in Discussion.

Methodology

HF Radar Network

These experiments were conducted within the New Jersey Shelf Observing System (Glenn & Schofield, 2002). A major component of this observing system is an HF radar network. The network was created in 1998 with the placement of two 25-MHz systems on the southern coastline of New Jersey (Kohut & Glenn, 2003). The network was then expanded with the placement of four 5-MHz systems spanning the New Jersey coastline (Gong et al., 2009). The 25-MHz network was moved north in 2003 in support of the Lagrangian Transport and Transformation Experiment (Chant et al., 2008). The work discussed here utilizes the latest addition to the network: the placement of a 13-MHz system outside the entrance to New York Harbor in Sea Bright, New Jersey. This network also contributes to the Mid-Atlantic Regional Coastal Ocean Observing System (MARCOOS), which has a total of 30 radars from Cape Hatteras to Cape Cod that are operated by eight universities (Roarty et al., 2010b).

13-MHz SeaSonde System

The radar was deployed in Sea Bright, New Jersey, 40 km south of the Battery in New York City. The radar was a direction-finding type radar, SeaSonde Remote Unit SSRS-100, manufactured by CODAR Ocean Sensors and was installed in October 2008. The radar's primary function was the measurement of surface currents, which are provided in real time to the NOAA National HF Radar Network (Temll et al., 2006). The radar also has the dual-use capability to detect the location of ships at sea.

The radar consists of a compact receive antenna with three elements: two directional crossed loops and an omnidirectional monopole, a monopole transmit antenna, and a hardware housed within a climate-controlled enclosure (Figure 1). The radar transmits a radio wave with a center frequency of 13.46 MHz and a bandwidth of 50 kHz. The bandwidth of the radar sets the spatial range resolution of the system, which was about 3 km for this particular bandwidth. The details of the waveform are given in Table 1. Separate transmit and receive antennas were used for this study spaced at least one wavelength apart, which is approximately 23 m at the 13-MHz radio band. A ship with a vertical structure of a quarter wavelength (6 m) is the minimum-sized optimal reflector (Ruck et al., 1970).

Figure 2 shows the spatial and temporal radial vector coverage for ocean currents of the radar over a 1-week period, which coincided with the ship detection exercise. The radar collected range data, which are a time series of the complex echo signal voltages before Doppler processing, from 00:00 GMT to 01:00 GMT on February 26, 2009. These range files are the result of the first fast Fourier transform

FIGURE 1

Picture of the (A) transmit antenna, (B) receive antenna, and (C) equipment enclosure for the SeaSonde 13-MHz radar.

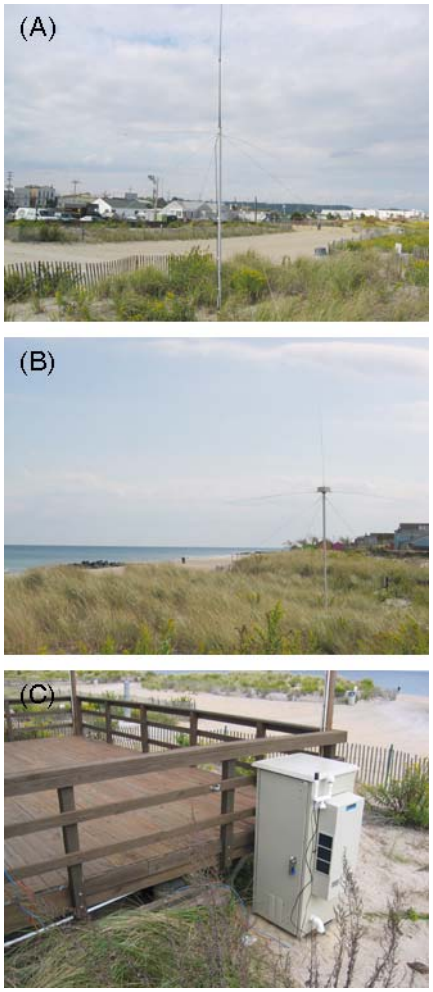

TABLE 1

Characteristics of the radar waveform used in the study.

Waveform Characteristic	Value
Center frequency	13.46 MHz
Bandwidth	50 kHz
Blank	668.8 µs
Blank delay	8.55 µs
Sweep rate	2 Hz
Pulse shaping	On

FIGURE 2

Radial coverage map of the SeaSonde at Sea Bright, New Jersey, over a 1-week period. The color map illustrates the temporal coverage along the radial grid (black = 75%, red = 50%, pink = 25%). (Color versions of figures available online at: http://www.ingentaconnect.com/content/mts/mtsj/2011/00000045/00000003.)

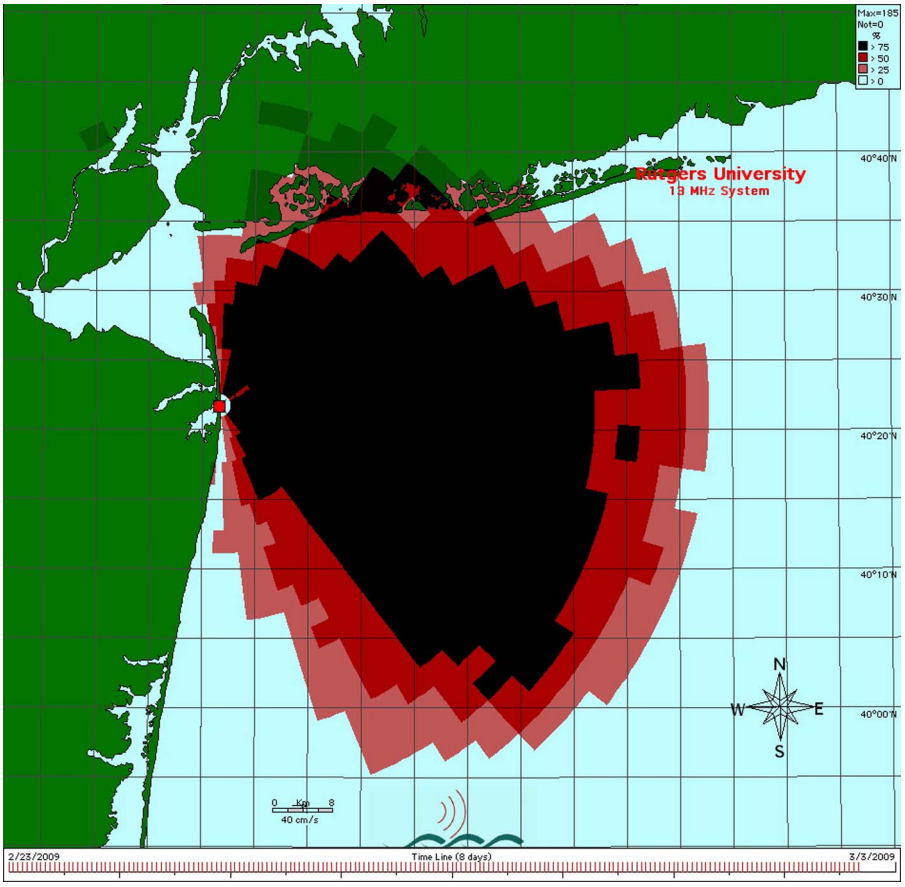

(FFT) of the frequency-modulated continuous wave received signal. The range data were collected using an FFT length of 512 points. With a 2-Hz sweep of the radar, each range file encompasses 256 s of coherent integration time. There were a total of 15 range files over the hour-long period. The time on the computer and all the subsequent files it generates are synchronized to atomic time via GPS by the Macintosh operating system.

AIS Receivers

Rutgers also operates an AIS receiver network, which was utilized in this study; this allows transponders on vessels to broadcast the ship's position and identification. When earlier work was performed (Roarty et al., 2010a), the authors were limited to verifying detections of vessels where a self-recording GPS could be placed on a vessel by the researchers or when the GPS information could be provided by other researchers (Rossby & Gottlieb, 1998). The ability of the researchers to obtain AIS position data on the vast majority of ships at sea has greatly accelerated the research. The Rutgers AIS network has receivers, which are manufactured by Shine Micro, Inc., located at its field station in Tuckerton, Sandy Hook, and Loveladies, New Jersey, as shown in Figure 3. The AIS transmissions are used as ground truth for the HF radar ship detections. The range of the shore-received AIS signal is typically 30 nautical miles, but under certain atmospheric conditions, range can be upwards of hundreds of nautical miles (International Maritime Organization, 2006). Data from the individual AIS receivers were sent back to the Rutgers Coastal Ocean Observation Laboratory (Glenn & Schofield, 2009), where it was archived using the Coast Guard software 'AIS Source.' The data were then time stamped using the clock on the computer. The computer kept time with a software tool to synchronize with the National Institute of Standards and Technology Internet Time Service. Figure 4 shows the tracks of vessels sent via AIS over a 3-week period, indicating that this is a target-rich environment and that vessels do not always stay in the shipping lanes.

Detection Software

The ship detection algorithm is explained in Roarty et al. (2010a). The ship detection code is written in the MATLAB programming language and is designed to run offline in a batch-processing mode. The range data that were collected by the radar were read by the software to process for the hard targets. The ship detection code utilizes a constant false alarm rate (CFAR) to find targets. A signal that is above the background by some threshold on the monopole and at least one of the two loops is considered a possible detection. Figure 5 shows the spectra from the monopole of the Sea Bright radar site at 00:15:21 GMT on February 26, 2009. The x axis denotes Doppler shift, the y axis shows signal strength, and the z axis denotes

FIGURE 3

Location of the three AIS receivers operated by Rutgers University shown as green circles. (Color versions of figures available online at: http://www.ingentaconnect.com/content/mts/mtsj/2011/00000045/00000003.)

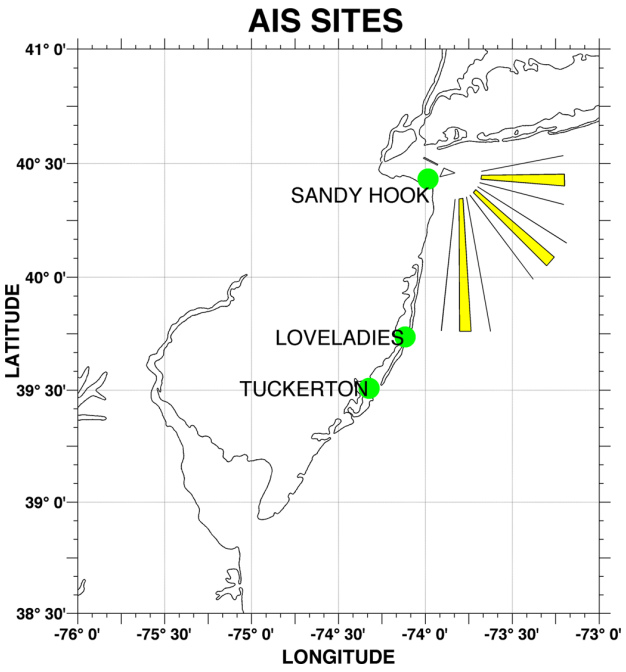

FIGURE 4

Map of the study area showing tracks of vessels (red lines) sent via AIS over a 3-week period. The Nantucket, Hudson Canyon and Barnegat (clockwise from right) shipping lanes are shown in the bottom right.

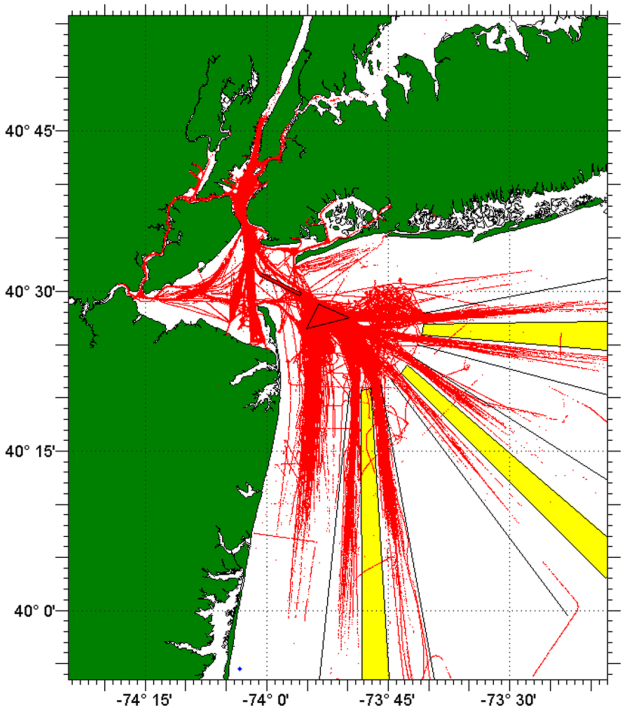

the radar range cell, which was 3 km for these spectra. The Bragg peaks from which surface currents are derived (Barrick, 1972) are shown ±0.4 Hz. The large signals at zero Doppler are signals returned to the radar from stationary objects. Ship signals can be seen between the Bragg peaks and the zero Doppler signals, with positive Doppler shift denoting a ship moving towards the radar and the corollary with a signal on the negative Doppler measuring a ship moving away from the radar. The ship detection code is designed to identify these signals. The code utilizes two schemes as the basis for thresholding in its CFAR peak-picking, where one averages in time, infinite impulse response (IIR), and the other averages in Doppler and range space using a median to create the signal background. In its current form, the code is able to process the data using three combinations of threshold and integration time for each background simultaneously. This results in a set of six detection packages after each software run. The detection code performs a sliding FFT on the range data so a new detection file is output every 32 s. This setting is adjustable so that the user can input the desired update rate for the detections. The output of the detection code is a series of files that contain range, range rate, and bearing of possible detections from the radar. The files also include the uncertainties in the above quantities, the signal-to-noise ratio for each antenna, and an estimate of the radar cross section of the possible target.

Results

The range data that were collected at the radar site were transported back

FIGURE 5

Picture of power spectra for Antenna 3 of the SeaSonde at 00:15 GMT on February 26, 2009. The *x* axis is Doppler shift (Hz), the *y* axis is signal strength (dB), and the *z* axis denotes the range bin from the radar (scalar). Vessel echoes are observed between the two sea-echo Bragg peaks at approximately ±0.4 Hz.

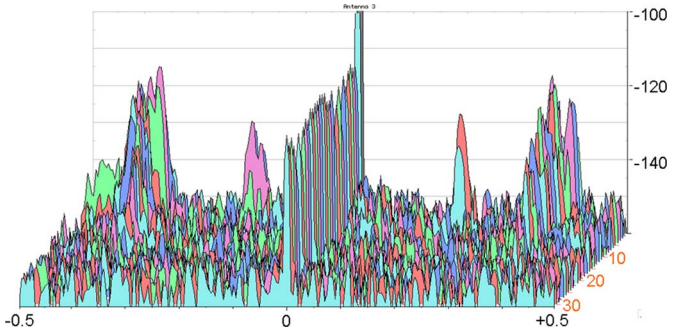

to the laboratory for offline processing. The user sets three combinations of integration time and threshold for each of the two backgrounds. Hence, the output of one run of the range data through the ship detection code results in six concurrent data streams of possible ship detections. Because the ship detection code only outputs six packages (three for the IIR method and three for the Median method) for each software run, the software is run several times to fill out our desired processing matrix. The threshold (dB)/FFT points that were initially tried using the IIR background were 6/16, 7/32, 8/64, 9/128, 10/256, and 11/512. The threshold (dB)/FFT points that were tried using the Median background were 8/32, 9/64, 10/128, 11/256, 12/512, and 13/1024. The threshold was increased because the average of signal to noise increased by ~1 dB for each doubling of the FFT length (Roarty et al., 2010a). A plot of range (km), range rate (m/s), and bearing (degrees clockwise from north) of possible detections using the IIR background, 256-point FFT, and 10-dB threshold is shown in Figure 6. The trails of vessels can be seen in the range and range rate subplots. There are also false positives in the data stream as noted by the single detections with no adjacent detections in space or time.

The AIS data were then used to see how the radar was performing when it came to detecting the speed and location of vessels at sea. The AIS data were first filtered by time to coincide with the measurements, then geographic proximity to the radar site (a 60-km threshold was used) and then binned by ship identification. Eighteen ships passed this first stage of filtering. Then any ship that was located on the bay side of the radar or had zero radial velocity was removed. This left four ships for possible detection, one tug boat (the *Dolphin*), two cargo containers (the *Maas Trader* and the *MOL Efficiency*), and a tanker (the *Joelmare*). The latitude, longitude, and time

FIGURE 6

Plot of target detections from 00:10 to 00:55 GMT on February 26, 2009. Panels from top to bottom are range, range rate, and bearing. The yellow horizontal lines in the middle are the expected positions of the very strong Bragg sea clutter echoes that would mask vessel detection.

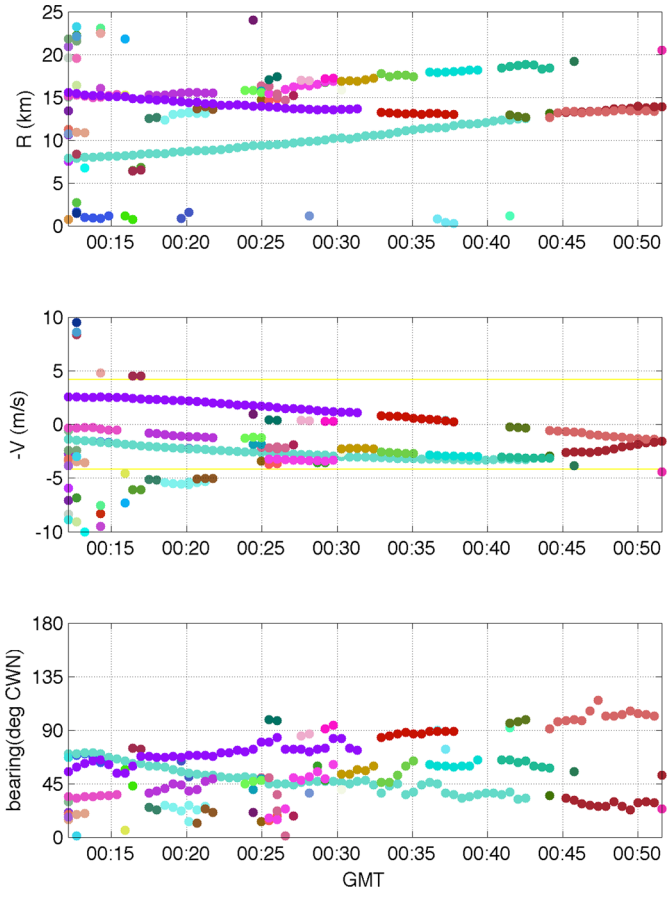

reports of these four ships were used to calculate the ship range, radial velocity, and bearing relative to the radar at Sea Bright, New Jersey. A text file of ship position and time was processed using the program 'GPSTracker', which is part of the SeaSonde detection software package. This software is normally used to perform the same task when measuring the antenna pattern of the receive antenna with a transponder on a vessel. This software generates a file for each vessel that contained the range, radial velocity, and bearing of that particular vessel as shown in Figure 7. These data were then used for comparison with the range, radial velocity, and bearing calculations from the radar.

The next step was to compare the data from the radar with data obtained via AIS. If the calculated range is within half the width of a range bin (1.5 km in this case) and within two Doppler bins (varied between 0.02 and 1.4 m/s, depending on the length of the FFT window) of the actual vessel, then the detection is considered a hit. A detection rate is then calculated as the number of times the radar detected the target divided by the total number of time sample possibilities, which was every 32 s for this experiment. The detection rates for *Joelmare* using the IIR and Median background are shown in Tables 2 and 3, respectively. The detection rates for *Maas Trader* using the IIR and Median background are shown in Tables 4 and 5, respectively. The detection rates for the *Dolphin* using the IIR and Median background are given in Tables 6 and 7, respectively. In the case of the *Maas Trader*, once the highest detection rate was found for the initial runs, then the thresholds were varied along the FFT length with the highest detection rate. The detection

FIGURE 7

Range, range rate, and bearing plot of four vessels in the vicinity of the Sea Bright HF radar station on February 26, 2009 as measured by AIS.

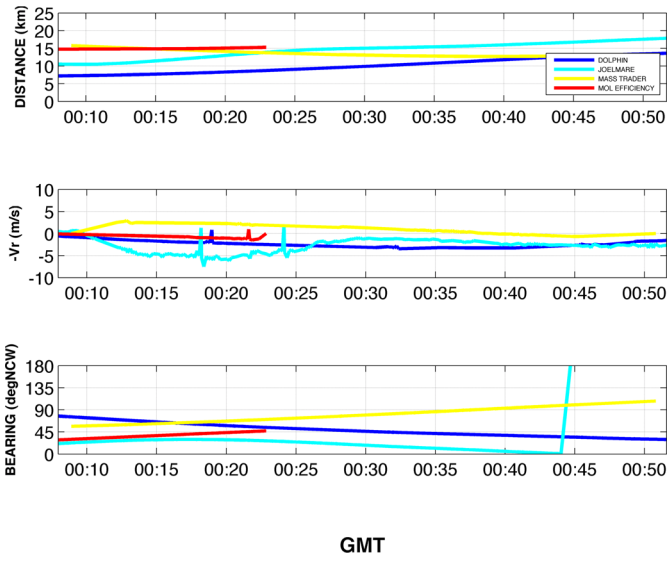

TABLE 2

Detection rate in percent for the *Joelmare* with different combinations of threshold (columns) and FFT points (rows) using the IIR background.

	6 dB	7 dB	8 dB	9 dB	10 dB	11 dB
16	NSD					
32		NSD				
64			0.6			
128				15.6		
256					13.2	
512						10.8

NSD stands for "no ship detected."

TABLE 3

Detection rate for the *Joelmare* with different combinations of threshold (columns) and FFT points (rows) using the Median background.

	8 dB	9 dB	10 dB	11 dB	12 dB	13 dB
32	0.2					
64		3.3				
128			34.0			
256				33.3		
512					12.5	
1024						7.6

TABLE 4

Detection rate in percent for the *Maas Trader* with different combinations of threshold (columns) and FFT points (rows) using the IIR background.

	6 dB	7 dB	8 dB	9 dB	10 dB	11 dB
16	NSD					
32		NSD				
64			NSD			
128				58.7		
256	70.3	70.3	68.9	66.2	64.9	64.9
512						38.5

NSD stands for "no ship detected."

TABLE 5

Detection rate for the *Maas Trader* with different combinations of threshold (columns) and FFT points (rows) using the Median background.

	8 dB	9 dB	10 dB	11 dB	12 dB	13 dB
32	13.8					
64		23.6				
128			55.0			
256	65.0	65.0	62.5	61.3	58.8	58.8
512					46.5	
1024						30.8

TABLE 6

Detection rate for the Tugboat *Dolphin* with different combinations of threshold (columns) and FFT points (rows) using the IIR background.

	6 dB	7 dB	8 dB	9 dB	10 dB	11 dB
16	NSD					
32		0.5				
64			5.4			
128				92.4		
256					73.1	
512						60.0

NSD stands for "no ship detected."

rate for the *MOL Efficiency* was not calculated due to a short AIS record, but there are results that will be discussed in the next section.

An example of the "association" of the detections with the ground truth data is shown in Figure 8. This figure shows the detections made by the radar associated with the GPS position of the cargo ship the *Maas Trader* from Figure 6. The detections are shown as blue diamonds with error boxes around the detection, with half the height signifying the uncertainty of the measurement and the width of the box denoting the length of the FFT window. The uncertainty σ is given by the equation

$$\sigma = \frac{\Delta}{\sqrt{\mathrm{SNR}_3}},$$

where Δ is the range, range rate, or bearing bin size and SNR_3 is the signal-to-noise ratio on Antenna 3 (the monopole). This figure is characteristic of the uncertainty provided by the SeaSonde HF radar that determines bearing using direction finding, i.e., low uncertainty in range and range rate measurements and higher uncertainty for the bearing estimate.

Discussion

We will now discuss detection results of the radar with four vessels that passed in front of the radar during the test period.

Cargo Container *MOL Efficiency*

The *MOL Efficiency*, International Maritime Organization (IMO) Ship No. 9251365, is a cargo container with a length of 294 m and a beam of 32 m. The vessel was exiting New York Harbor on a southeast course

TABLE 7

Detection rate for the Tugboat *Dolphin* with different combinations of threshold (columns) and FFT points (rows) using the Median background.

	8 dB	9 dB	10 dB	11 dB	12 dB	13 dB
32	10.8					
64		31.0				
128			93.2			
256				78.6		
512					56.2	
1024						32.8

and was approximately 15 km from the radar. The AIS record of the *MOL Efficiency* only spans from 00:00 to 00:23 GMT on February 26, 2009. It is unclear to the authors as to why the AIS record terminated.

FIGURE 8

Plot of target detections (blue dots) and corresponding uncertainty values (blue squares) associated with GPS track of the *Maas Trader* (solid aqua line). The panels from top to bottom are range (km), radial velocity (m/s), and bearing (degrees clockwise north). The uncertainty values for each measurement are shown as the height of each blue box; the length of the FFT is the width of the box. (Color versions of figures available online at: http://www.ingentaconnect.com/content/mts/mtsj/2011/00000045/00000003.)

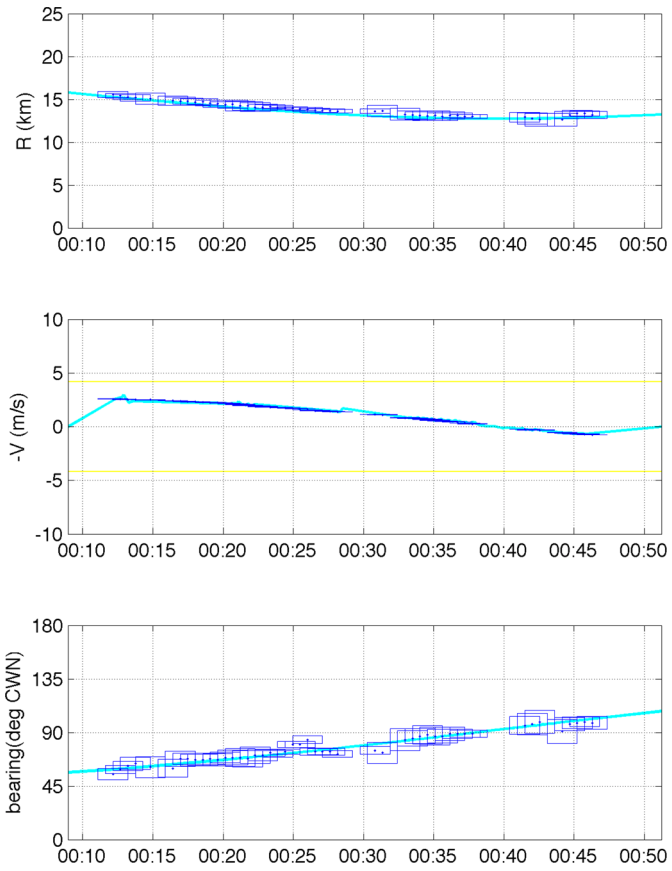

Did the operators of the vessel stop transmitting the signal, or were the receivers unable to record the signal? The radar was able to make detections on the vessel coincidental with the AIS data. If we assume that the vessel maintained its course and the radial velocity maintained its rate of change, then the radar did indeed make the additional detections of the vessel as clearly shown in Figure 9.

Tanker *Joelmare*

The *Joelmare*, IMO Ship No. 9288019, is a tanker with a length of 228 m and a beam of 32 m. The tanker *Joelmare* was exiting New York Harbor but then turned around and headed back into the harbor. The radar was able to detect the vessel 34% of the time with the Median background and 16% of the time using the IIR background. We propose two explanations as to why the radar did not detect this vessel very well. First, from Figure 7: The radial velocity of the vessel was noisiest of all the vessels. This lack of a constant radial velocity would spread the energy of the returned signal over several Doppler bins. This would cause the signal to not be detected, because its amplitude falls below the threshold set in the software. The second reason as to why the radar did not detect this vessel was that the vessel was north-northeast of the radar site, and the signal had to propagate over large sections of land that attenuated the signal in those directions.

Cargo Container *Maas Trader*

The *Maas Trader*, IMO Ship No. 9308625, has a length of 139 m, a beam of 23 m, and a gross tonnage of 9981. More particulars on this vessel as well as the *Dolphin* are given in Table 8.

FIGURE 9

Plot of target detections for range, range rate, and bearing. The solid aqua line from 00:10 to 00:23 GMT shows the path of the *MOL Efficiency* from the AIS signal. There are additional detections past 00:23 on the figure, but the AIS data were not available to compare with the radar detections. (Color versions of figures available online at: http://www.ingentaconnect.com/content/mts/mtsj/2011/00000045/00000003.)

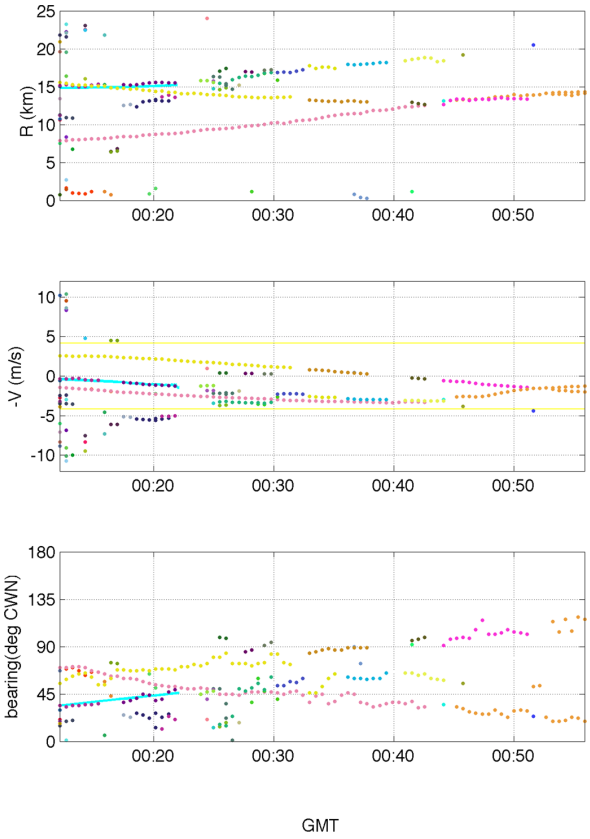

TABLE 8

Characteristics of vessels detected in this study.

Vessel Characteristic	*Maas Trader*	*Dolphin*	*MOL Efficiency*	*Joelmare*
MMSI No.	237956000	366920980	351166000	477738400
IMO No.	9308625	7319010	9251365	9288019
Type	Cargo	Tug	Cargo	Tanker
Length (m)	139	41	294	228
Beam (m)	23	6	32	32
Hull type	Single	Single	NA	NA
Gross tonnage	9981	198	NA	NA
Depth (m)	11.8	5	NA	NA
Draught (m)	8	4.25	12.1	6.6
Freeboard (m)	3	0.75	NA	NA
Hull material	Steel	Steel	NA	NA

NA stands for "not available."

The authors were unable to find the height above the water for any of the vessels detected. The cargo container *Maas Trader* was heading south in the Barnegat shipping lane for this test. The radar at Sea Bright had the best detection rate of 70% using the IIR background and 65% with the Median background. Both of these cases occurred with the lowest threshold and yielded the highest number of false positives. It would be up to a potential user of the detection files to determine where the threshold should be set. If the detection files were to be passed on to a tracker, the performance of the data in the tracker could help determine what the threshold level should be. Another option is to run all combinations of FFT length and threshold and let a tracker determine which detections are authentic and which ones are false. The radar was not able to detect the vessel at 00:40. This was due to the fact that the vessel was crossing through the zero Doppler area, where there are large echoes from stationary objects. A plot of the FFT length and threshold combinations versus detection rate, which is a summary of Tables 4 and 5 for the *Maas Trader* test case, is given in Figure 10. A peak in the detection rate is found between the 128- and 256-point FFT. With a 2-Hz sweep, this converts to a 1- to 2-min averaging period as optimal for the detection of these vessels with the HF radar.

Tugboat *Dolphin*

The *Dolphin*, IMO Ship No. 7319010, has a length of 41 m, a beam of 10 m, and a gross tonnage of 198. The tugboat *Dolphin* was heading north into New York Harbor inside of the Barnegat shipping lane. Figure 4 shows that this is a heavily transited

FIGURE 10

Response of detection rate to the variance of FFT length and threshold level.

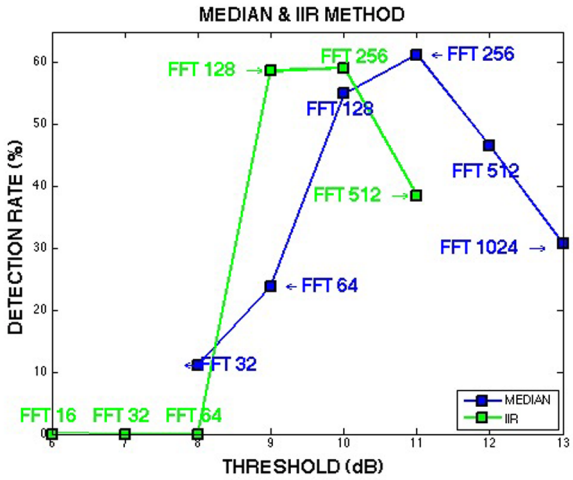

route as well. The Sea Bright radar had the highest detection rate on this vessel with a 92% using the IIR background and 93% using the Median background. The vessel had a large superstructure, which made it an ideal target for the radar. The best case detections from the *Dolphin* and *Maas Trader* were placed on a map in Figure 11.

FIGURE 11

Detections of the *Maas Trader* (IIR background, 256-point FFT, and 10-dB threshold) and *Dolphin* (median background, 256-point FFT, and 10-dB threshold) overlaid on the path of the vessel from GPS/AIS.

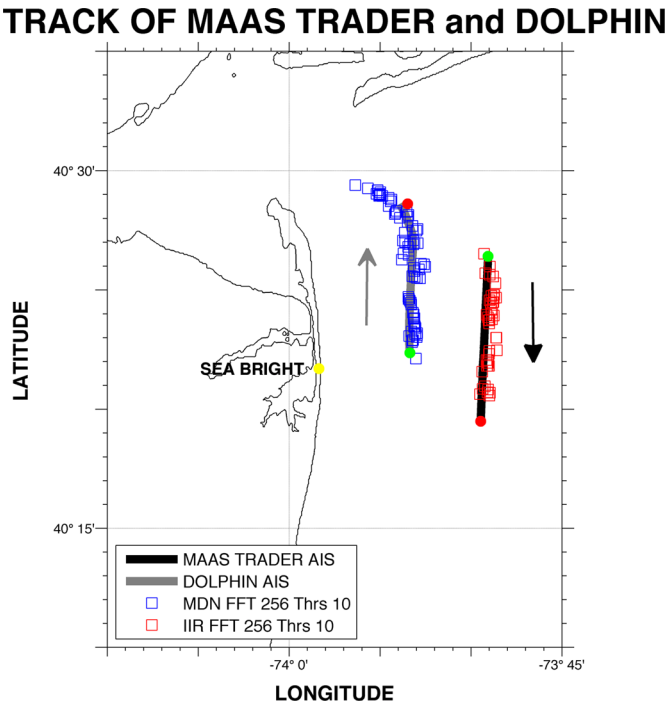

Summary

A case study has been performed using a SeaSonde HF radar to detect vessels at sea in a dual-use mode. The selected 13-MHz HF radar that operates within the MARCOOS and provides radial current data to the NOAA National HF Radar Network simultaneously detected the speed and location of several ships at sea. The detections made with the HF radar were checked against the GPS position of the target sent via the AIS system. An optimal integration time for this type of radar with this class of vessel is between 1 and 2 min. The detection rates for some vessels were above 90%. Lower thresholds resulted in higher detection rates but also led to higher false alarm rates. Overall, the median background performed better than the IIR background, but there were instances where the IIR background was the best.

One benefit of HF systems for vessel detection/tracking is that they provide over-the-horizon detection capability (Khan et al., 1994). The systems being developed and evaluated within the 5-MHz and 13-MHz bands regularly see vessels between 50 and 110 km. However, the focus of this paper was on the optimal processing parameters that would enable the best detections. Because of this, the authors focused on vessels that were close to shore and would provide the most signal to test these parameters without introducing other parameters from the radar equation. The authors will, in future work, use these optimal parameters to test the range limits of the vessel detection system as a separate study.

A significant finding was that the same targets were seen by the detection algorithm simultaneously, at different

FFT/coherent-integration times, with different thresholding and backgrounds. Thus, one is not forced to preselect a fixed processing parameter suite. A properly optimized association algorithm (which is under development) would search for detections of the same vessel among all of the output combinations and thereby yield a much improved detection. This would increase the detection rate seen by an individual look of 90%, for example, to perhaps 98%, while reducing the overall false alarm rate.

This offers the opportunity to convert the National HF Radar Network into a dual-use system that would provide surface currents to the U.S. Coast Guard as well as provide wide area surveillance in the maritime domain to the Department of Homeland Security.

Acknowledgment

This material is based on work supported by the U.S. Department of Homeland Security under Award No. 2008-ST-061-ML0001.

The views and conclusions contained in this document are those of the authors and should not be interpreted as necessarily representing the official policies, either expressed or implied, of the U.S. Department of Homeland Security.

Lead Author:

Hugh J. Roarty
Coastal Ocean
Observation Laboratory
Institute of Marine and
Coastal Sciences
Rutgers University
New Brunswick, NJ 08901
Email: hroarty@marine.rutgers.edu

References

Barrick, D. 1972. First-order theory and analysis of MF/HF/VHF scatter from the sea. IEEE Trans Antennas Propag. 20(1):2-10. doi: 10.1109/TAP.1972.1140123.

Chant, R.J., Glenn, S.M., Hunter, E., Kohut, J., Chen, R.F., Houghton, R.W., … Schofield, O. 2008. Bulge formation of a buoyant river outflow. J Geophys Res. 113(C1):C01017.

Department of Homeland Security Science and Technology. 2009. High-Priority Technology Needs. Washington, D.C. 24 pp. Available at: http://www.dhs.gov/xlibrary/assets/st_high_priority_technology_needs.pdf.

Glenn, S.M., & Schofield, O. 2009. Growing a distributed ocean observatory: Our view from the COOL room. Oceanography. 22(2):128-45.

Glenn, S.M., & Schofield, O.M.E. 2002. The New Jersey shelf observing system. OCEANS '02 MTS/IEEE. 3:1680-7.

Gong, D., Kohut, J.T., & Glenn, S.M. 2009. Seasonal climatology of wind-driven circulation on the New Jersey shelf. J Geophys Res. 109(C7):C07S07.

Interagency Working Group on Ocean Observation. 2009. A Plan to Meet the Nation's Needs for Surface Current Mapping. Washington, D.C. 64 pp.

International Maritime Organization. 2006. Automatic Identification Systems. London: IMO Publishing. 102 pp. Available at: http://www.ioos.gov/library/surfacecurrentplan9_3lowres.pdf.

Khan, R., Gamberg, B., Power, D., Walsh, J., Dawe, B., Pearson, W., & Millan, D. 1994. Target detection and tracking with a high frequency ground wave radar. Journal of Oceanic Engineering. 19(4):540-8.

Kohut, J.T., & Glenn, S.M. 2003. Improving HF radar surface current measurements with measured antenna beam patterns. J Atmos Oceanic Technol. 20(9):1303-16. doi: 10.1175/1520-0426(2003)020<1303:IHRSCM>2.0.CO;2.

Roarty, H.J., Barrick, D.E., Kohut, J.T., & Glenn, S.M. 2010a. Dual-use compact HF radars for the detection of mid- and large-size vessels. Turk J Electr Eng Comput Sci. 18(3):373-88.

Roarty, H.J., Glenn, S.M., Kohut, J.T., Gong, D., Handel, E., Rivera Lemus, E., … Seim, H. 2010b. Operation and application of a regional high-frequency radar network in the Mid-Atlantic Bight. Mar Technol Soc J. 44(6):133-45.

Rossby, T., & Gottlieb, E. 1998. The Oleander Project: Monitoring the variability of the gulf stream and adjacent waters between New Jersey and Bermuda. Bull Am Meteorol Soc. 79:5-18. doi: 10.1175/1520-0477(1998)079<0005:TOPMTV>2.0.CO;2.

Ruck, G.T., Barrick, D.E., Stuart, W.D., & Krichbaum, C.K. 1970. Radar Cross Section Handbook. New York: Plenum Press. 949 pp.

Temll, E., Otero, M., Hazard, L., Conlee, D., Harlan, J., Kohut, J., … Lindquist, K. 2006. Data management and real-time distribution in the HF-radar national network. In: OCEANS 2006 MTS/IEEE Proceedings, pp. 1-6. Boston, MA. doi: 10.1109/OCEANS.2006.306883.